

# Electrical transport and carrier density collapse in doped manganite thin films

L. M. Wang,<sup>1</sup> H. C. Yang,<sup>2</sup> and H. E. Horng<sup>3</sup>

<sup>1</sup>*Department of Electrical Engineering, Da-Yeh University, Chang-Hwa 515, Taiwan*

<sup>2</sup>*Department of Physics, National Taiwan University, Taipei 106, Taiwan*

<sup>3</sup>*Department of Physics, National Taiwan Normal University, Taipei 117, Taiwan*

(Received 30 July 2001; published 21 November 2001)

Based on the current-carrier-density-collapse theory, an expression is proposed for resistivity as a function of temperature and magnetic field. Our low-temperature resistivity data on high-quality epitaxial thin films of doped Mn oxides can be well fitted by the derived equation. At temperatures above  $T_c$ , the zero-field resistivity data can be also well explained by the carrier-density-collapse model. Moreover, the features of electrical transport in doped Mn oxides such as a dominant  $T^2$  dependence of low-temperature resistivity, and a strong  $H^2$  dependence of magnetoresistance at temperatures above  $T_c$  are successfully interpreted in accordance with our deduction. We provide strong evidence to support that the carrier-density collapse can well describe the electrical transport in doped manganites.

DOI: 10.1103/PhysRevB.64.224423

PACS number(s): 75.30.Vn, 71.30.+h, 71.38.Mx, 72.10.-d

## I. INTRODUCTION

In recent years, the magnetotransport properties of the magnetic compounds  $R_{1-x}A_x\text{MnO}_3$  ( $R=\text{La, Nd, Pr}$  and  $A=\text{Ca, Sr, Ba, Pb}$ ) have been a subject of great interest. Earlier reports showed that these manganites undergo a transition from paramagnetic (PM) insulator to ferromagnetic (FM) metal associated with a colossal magnetoresistance (CMR) effect.

However, the electrical transport mechanism for the Mn oxides is still unclear both at FM and PM states. At low temperatures, a dominant  $T^2$  contribution in resistivity is generally observed.<sup>1,2</sup> The  $T^2$  behavior has been ascribed to electron-electron scattering,<sup>1</sup> while a single-magnon scattering mechanism has been proposed by Jaime *et al.*<sup>3</sup> Recently, Akimoto, Moritomo, and Nakamura<sup>4</sup> observed a  $T^3$  dependence of resistivity in some manganites and interpreted this behavior in terms of an anomalous single-magnon scattering process. Additionally, a  $T^{4.5}$  term contributed from two-magnon scattering also has been taken into account in the low-temperature regime,<sup>2,4</sup> even if it is small. Otherwise, for  $T$  above  $T_c$ , the resistivity data on the manganites have been fitted to some models such as a simple Arrhenius law,<sup>5</sup> a polaron model,<sup>6</sup> and a variable-range hopping model.<sup>7</sup> Nevertheless, the full information of resistivity for  $T$  near  $T_c$  seems to be lacking, although several theoretical studies have been made on the insulator-metal transition in the manganite.<sup>8,9</sup> Thus, there is a further point that needs to be clarified both in experimental and theoretical work.

Recently, in a theory of Alexandrov and Bratkovsky (AB),<sup>10</sup> polarons are considered as the carriers even in the low-temperature metallic state. Their model predicts that the bipolarons form in the paramagnetic phase and undergo a breakdown of a bipolaron into two polaronic carriers when the temperature is below  $T_c$ . The current-carrier-density-collapse (CCDC) model has been strongly supported by the oxygen-isotope effects on the intrinsic resistivity and thermoelectric power in several ferromagnetic manganites,<sup>11,12</sup> and partially supported by the low-temperature optical data.<sup>13</sup> According to the assumption of small-polaron trans-

port mechanism, Zhao *et al.*<sup>14</sup> have shown that the behavior of resistivity below 100 K is consistent with small-polaron coherent motion that involves a relaxation due to a low-lying optical phonon mode. However, only according to the theory of AB, large differences exist between the experimental and theoretical curves as shown in their work.<sup>15</sup> A similar case is observed also in the Ti-doping manganites.<sup>16</sup> Thus a phenomenological model that seems to fit the resistance data for both the PM and FM states has been proposed by Yuan *et al.*<sup>17</sup> However, a strict theoretical account for the transport origin seems to be lacking in their assumption. In this paper, we advance an expression of resistivity to explain the electrical transport behavior for the manganites based on the CCDC model. Here we propose a view of the electric transport in the doped-manganite perovskites based on the CCDC theory, and provide a strong experimental evidence to support it. Some of the features of electric transport in manganites are discussed and interpreted in accordance with our proposition.

## II. MODEL AND FORMULATION

We derive the resistivity function from the CCDC model. In this model, the carrier density  $n$  of single (unbound) hole polarons and the normalized magnetization  $\sigma$  of  $\text{Mn}^{3+}$  ions can be obtained by the following equations:<sup>10</sup>

$$n = 2\nu y \cosh[(\sigma + h)/t], \quad (1)$$

and

$$y^2 = (x - n)/(2\nu)^2 \exp(-2\delta/t). \quad (2)$$

Here, the dimensionless temperature  $t = 2k_B T/J_{pd}S$ ; the magnetic field  $h = 2\mu_B H/J_{pd}S$ ; and the binding energy  $\delta \equiv \Delta/J_{pd}S$ , in which  $\Delta$  is the bipolaron binding energy,  $J_{pd}S$  is the exchange interaction of  $p$  holes with four  $d$  electrons of the  $\text{Mn}^{3+}$  ion,  $x$  is a constant that represents the doping concentration, and  $\nu = 3$  is the degeneracy of the  $p$  band.

Substituting Eq. (2) into Eq. (1), we can obtain the quadratic equation:  $n^2 + 2 \cosh^2[(\sigma+h)/t]e^{-2\delta/t}n - 2x \cosh^2[(\sigma+h)/t]e^{-2\delta/t} = 0$ . Therefore, by solving this equation, we have the solution of  $n$ ,

$$n = e^{-\delta/t} \cosh[(\sigma+h)/t] \left\{ \left[ e^{-2\delta/t} \cosh^2((\sigma+h)/t) + 2x \right]^{1/2} - e^{-\delta/t} \cosh[(\sigma+h)/t] \right\}. \quad (3)$$

Furthermore, as demonstrated by Zhao *et al.*,<sup>14</sup> at low

$$\rho - \rho_0 = A \frac{1}{\sinh^2(\hbar\omega_s/2k_B T)} \frac{e^{\delta/t}}{\cosh\left(\frac{\sigma+h}{t}\right) \left\{ \left[ e^{-2\delta/t} \cosh^2\left(\frac{\sigma+h}{t}\right) + 2x \right]^{1/2} - \cosh\left(\frac{\sigma+h}{t}\right) e^{-\delta/t} \right\}}, \quad (4)$$

where  $A$  is a constant, being proportional to the effective mass of polarons.

On the other hand, for  $T > T_c$  and in zero magnetic field, one can easily find that  $n$  is dominantly dependent on the term of  $\exp(-\Delta/2k_B T)$  as shown in Eq. (3). In the regime of adiabatic small-polaron hopping, the mobility of the carriers is given by  $\mu \propto (1/k_B T) \exp(-E_a/k_B T)$ , where  $E_a$  is the energy related to the polaron formation energy and the electronic transfer integral.<sup>18</sup> Taking account of  $\rho = 1/ne\mu$ , we obtain the zero-field resistivity as

$$\rho = CT \exp(E_p/k_B T), \quad (5)$$

where  $E_p$  is the activation energy related to the bipolaron binding energy and the polaron-formation energy; and  $C$  a prefactor. This expression has been regarded as the small polaron hopping model.<sup>6,19</sup> Besides, a modified form of Eq. (5),  $\rho = C/\sqrt{T} \exp(E_p/k_B T)$ , was derived by Zhao *et al.*,<sup>11</sup> in which a different prefactor from that of Eq. (1) was considered for a finite polaron bandwidth.

Based on Eqs. (4) and (5), the temperature dependence of resistivities for our doped-manganite thin films is examined below.

### III. RESULTS AND DISCUSSION

Epitaxial thin films of doped manganites were grown on SrTiO<sub>3</sub>(100) substrates by the off-axis magnetron sputtering technique. A detailed description of the experiments has been reported elsewhere.<sup>20</sup> Four samples, Nd<sub>0.7</sub>Sr<sub>0.3</sub>MnO<sub>3</sub> thin films grown at 770 °C (NSMOa) and at 720 °C (NSMOb), La<sub>0.7</sub>Ca<sub>0.3</sub>MnO<sub>3</sub> thin film grown at 720 °C (LCMO), and La<sub>0.7</sub>Sr<sub>0.3</sub>MnO<sub>3</sub> thin film grown at 720 °C (LSMO) were used in this study. Figure 1 shows the temperature dependence of resistivities in  $H=0$  and 7 T for the four samples. All the  $\rho$ - $T$  curves are similar to that reported by others and show a small residual resistivity. The resistivity values are slightly larger than that reported for single-crystal samples,<sup>21,22</sup> indicating that the quality of our films is good and the impurity effect is negligible. Also shown in the insets of Fig. 1 are the

temperature dependence of negative magnetoresistance (MR) ratio,  $-\Delta\rho$ , defined as  $-\Delta\rho = [\rho(0) - \rho(7 \text{ T})]/\rho(7 \text{ T})$ , for the four samples. It can be seen that a maximum magnitude of MR ratio  $-\Delta\rho_{\text{max}}$  occurs in all the films. The values of  $-\Delta\rho_{\text{max}}$  are 2700, 770, 1100, and 62%, respectively, for NSMOa, NSMOb, LCMO, and LSMO films, which occur at temperatures of 160, 205, 220 and 330 K, respectively. It is known that the highest peak temperature  $T_p$  of MR corresponds to its FM transition temperature.

First, we examine the  $\rho$ - $T$  behavior in the FM state. For  $T$  below  $T_c$ , Eq. (4) is used to fit the  $\rho$ - $T$  curves. The condition of  $k_B T < 2t_p$ , however, must be checked before fitting. The hopping integral of polarons  $t_p$  can be estimated approximately. By using Eq. (1) shown in Ref. 14,  $\rho = (\hbar^2/ne^2 a^2 t_p)(1/\tau)$ , and the expression of  $\rho = m^*/ne^2\tau$ ,

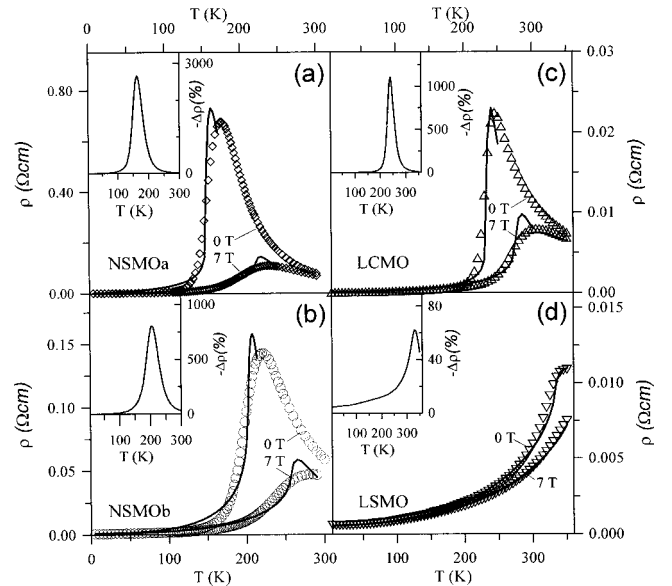


FIG. 1. Temperature dependence of resistivities for (a) NSMOa, (b) NSMOb, (c) LCMO, and (d) LSMO films. Solid lines are the fitted curves by Eq. (6). Insets: Temperature dependence of the MR ratio for the corresponding samples.

then we can obtain  $t_p = \hbar^2/a^2m^*$ . Values of  $m^*$  could be estimated using other experimental techniques, such as optical spectroscopy and specific-heat measurements. The values of effective mass are taken by  $m^* \approx 21m_e$ ,  $13m_e$  and  $4m_e$  for  $\text{Nd}_{0.7}\text{Sr}_{0.3}\text{MnO}_3$ ,<sup>21</sup>  $\text{La}_{0.7}\text{Ca}_{0.3}\text{MnO}_3$ ,<sup>23</sup> and  $\text{La}_{0.7}\text{Sr}_{0.3}\text{MnO}_3$  [Ref. 22], respectively, where  $m_e$  is the electron mass. Taking the lattice constant of manganites,  $a \approx 3.9 \text{ \AA}$ , we obtain the values of  $t_p$  as  $t_p \approx 277$ ,  $447$ , and  $1454 \text{ K}$  for  $\text{Nd}_{0.7}\text{Sr}_{0.3}\text{MnO}_3$ ,  $\text{La}_{0.7}\text{Ca}_{0.3}\text{MnO}_3$ , and  $\text{La}_{0.7}\text{Sr}_{0.3}\text{MnO}_3$ , respectively. Thus the condition of  $k_B T < 2t_p$  is confirmed for the analysis of low-temperature data.

In using Eq. (4), we can take the experimental magnetization data as  $\sigma = M/M_{\text{max}}$ , where  $M_{\text{max}}$  is the maximum magnetization, as in Liu, Xu, and Zhang.<sup>16</sup> Figure 2 shows the temperature dependence of magnetization

$M/M(5 \text{ K})$  in field of 100 G for the four samples. We find that as  $T \rightarrow T_c$  from below, the magnetization becomes proportional to  $(1 - T/T_c)^\beta$  for the samples, where  $\beta \approx 0.33 \pm 0.02$ . Our results generally agree with the observation in  $\text{La}_{0.67}\text{Ca}_{0.33}\text{MnO}_3$ , indicating a second-order phase transition occurring on our samples.<sup>24</sup> It is also found that the power  $\beta$  is weakly dependent on the applied field as shown in the inset of Fig. 2. Thus the temperature dependence of  $\sigma$  could be described by  $\sigma \propto (1 - T/T_c)^\beta$ . Here we need scarcely add that the effect of deviation between fitting curves and data at temperatures near zero as shown in Fig. 2 is considerably neglected because the equation of carrier density  $n$ , Eq. (3), is approximately independent on temperature when  $T$  is far below  $T_c$ .<sup>10</sup> So far, we can see that in the absence of magnetic field Eq. (4) can be rewritten as

$$\rho - \rho_0 = A \frac{1}{\sinh^2\left(\frac{\lambda_4}{2T}\right)} \frac{1}{\cosh\left[\frac{\lambda_2(1 - T/\lambda_3)^{0.33}}{2T}\right]} \times \frac{\exp(\lambda_1/2T)}{\left\{ \sqrt{\exp(-\lambda_1/T) \cosh^2\left[\frac{\lambda_2(1 - T/\lambda_3)^{0.33}}{2T}\right]} + 2x - \cosh\left[\frac{\lambda_2(1 - T/\lambda_3)^{0.33}}{2T}\right] \exp(-\lambda_1/2T) \right\}}, \quad (6)$$

where  $\lambda_1$ ,  $\lambda_2$ ,  $\lambda_3$ , and  $\lambda_4$ , are the fitting parameters and they correspond to the bipolaron binding energy, the product of  $J_{pd}S$  and the normalized magnitude of zero-temperature magnetization, the transition temperature, and  $\hbar\omega_S$ , in which  $\lambda_1$ ,  $\lambda_2$ ,  $\lambda_3$ , and  $\lambda_4$  are all in units of K. Here the residual resistivity  $\rho_0$  can be estimated by extrapolation of the  $\rho$ - $T$  curve,  $x=0.3$  is the doping concentration, and  $A$  is a free parameter.

As shown in Fig. 1, using Eq. (6) we can well fit the zero-field resistivity data for the four samples. The values of fitting parameters are listed in Table I. For resistivity in the presence of applied field, Eq. (6) still holds since the value of  $\mu_B H$  is so small that it is incomparable to  $\lambda_2$  (taking  $H = 7 \text{ T}$ ,  $\mu_B H \approx 4.7 \text{ K}$ ). In Eq. (6), only the parameters  $\lambda_2$  and  $\lambda_3$  are expected to be field dependent. Therefore, we fix the values of  $\lambda_1$  and  $\lambda_4$  to reduce the number of fitting parameters and change the values of  $\lambda_2$  and  $\lambda_3$  to fit the resistivity data. Figures 3(a) and 3(b) show the temperature dependence of resistivities in magnetic fields and the fitting curves for NSMOa and NSMOb samples, respectively. The fitting curves for LCMO and LSMO in  $H = 7 \text{ T}$  are also shown in Figs. 1(c) and 1(d), respectively. The agreement between the experimental data and theoretical calculating look quantitatively good for temperatures far below  $T_c$ . It is also found that the fitting curves deviate from the experimental data at temperatures close to  $T_c$ . The reason for this is not hard to see, that when the temperature is close to  $T_c$ , the magnitude of magnetization will decrease drastically, so the term of

$\mu_B H$  needs to be considered. Part of the fitting parameters,  $\lambda_2(7 \text{ T})$  and  $\lambda_3(7 \text{ T})$  for NSMOa and NSMOb samples are also shown in Table I. It is noticed that the  $\lambda_2(7 \text{ T})$  value, which is defined by  $\lambda_2(7 \text{ T}) = J_{pd}S \times M(0 \text{ K}, 7 \text{ T})/M_{\text{max}}$ , is approximately equal to  $J_{pd}S$  because  $M/M_{\text{max}} \approx 1$  for the zero temperature and high fields. Then the  $J_{pd}S$  values are estimated to be 1410, 1672, 2120, and 1860 K for NSMOa, NSMOb, LCMO, and LSMO samples, respectively. It is found that the  $J_{pd}S$  values for our samples are comparable to that of 1000–2600 K for Ti-doping manganites<sup>16</sup> and consistent with that of 130 meV ( $\approx 1510 \text{ K}$ ) for the  $\text{La}_{0.7}\text{Ca}_{0.3}\text{MnO}_3$  film reported by Zhao *et al.*<sup>11</sup>

It can be seen that the value of  $\lambda_1$  for LSMO as shown in Table I is smaller than that for the others, implying a lower bipolaron binding energy for LSMO. It has been argued that the binding energy will decrease with an increase of  $T_c$ .<sup>25</sup> In addition, it is found that the parameters  $\lambda_2$  and  $\lambda_3$  get larger as the applied field is increased. This is due to the fact that the magnetization increases and  $T_c(H)$  shifts to higher temperature with an increase of magnetic field.

According to Eq. (6), we can see that at temperatures far below  $T_c$ , the resistivity will be dominated by the  $\sinh^{-2}(\lambda_4/2T)$  term because of the weak temperature dependence of  $n$ . Therefore, for  $T_c > T \gg \lambda_4/2$ , i.e.,  $T \gg 18$ – $42 \text{ K}$  for our samples, the sinh term can be linearized and a dominant  $T^2$  dependence of resistivity is expected. A strong  $T^2$  dependence of resistivity above 50 K has been reported by Jaime *et al.*<sup>3</sup> Agreement with the experiment supports the idea that

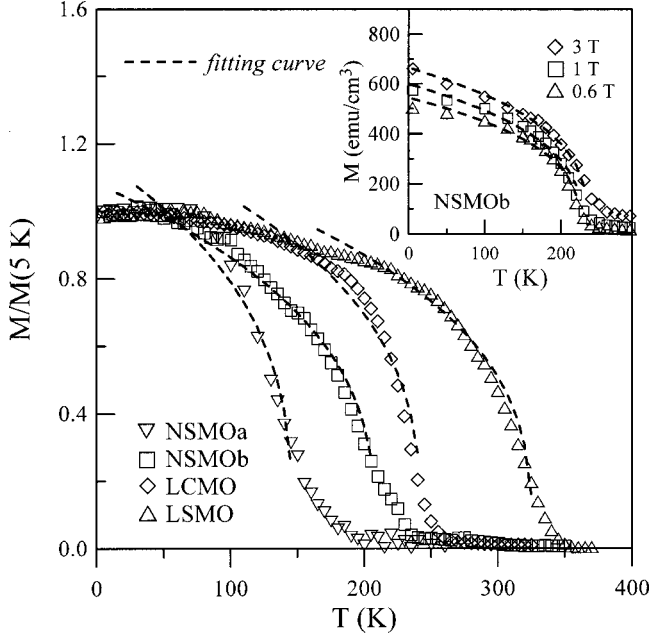


FIG. 2. Magnetization of various samples in  $H=100$  G. The dashed lines are the fitted curves by  $M \propto (1-T/T_c)^\beta$  with  $\beta = 0.33 \pm 0.02$ . The inset shows the magnetization of NSMOb sample in  $H=0.6, 1,$  and  $3$  T.

the  $T^2$  dependence of the resistivity at low temperature is due primarily to CCDC. The dominant  $\sinh^{-2}(\lambda_4/2T)$  dependence of the low-temperature resistivity has been also clarified by Zhao *et al.*<sup>14</sup>

To study the resistivity in the PM regime, the zero-field resistivity curves were fitted by using Eq. (5). Figures 4(a), 4(b), and 4(c) show the zero-field resistivities of NSMOa, NSMOb, and LCMO for  $T > 1.1T_p$ , respectively. As a result, the correspondence between the experimental data and the fitting curves is good. The values of  $E_\rho$  are also listed in Table I. This result is similar to that observed in other manganites<sup>19</sup> and supports the validity of our deduction. Moreover, it is found that the high-temperature resistivity data can be also well fitted by the modified equation,  $\rho = C/\sqrt{T} \exp(E_\rho/k_B T)$ . In this fit, the values of activation energy are 938, 712, and 811 K for NSMOa, NSMOb, and LCMO samples, respectively, which are smaller than that obtained from our previous fit.

Finally, we investigate the MR effect in the PM regime. For  $T > T_c$ , a  $\text{MR} \propto (M/M_s)^2$  behavior has been observed in several Mn oxides,<sup>1,26,27</sup> where  $M_s$  is the saturated magneti-

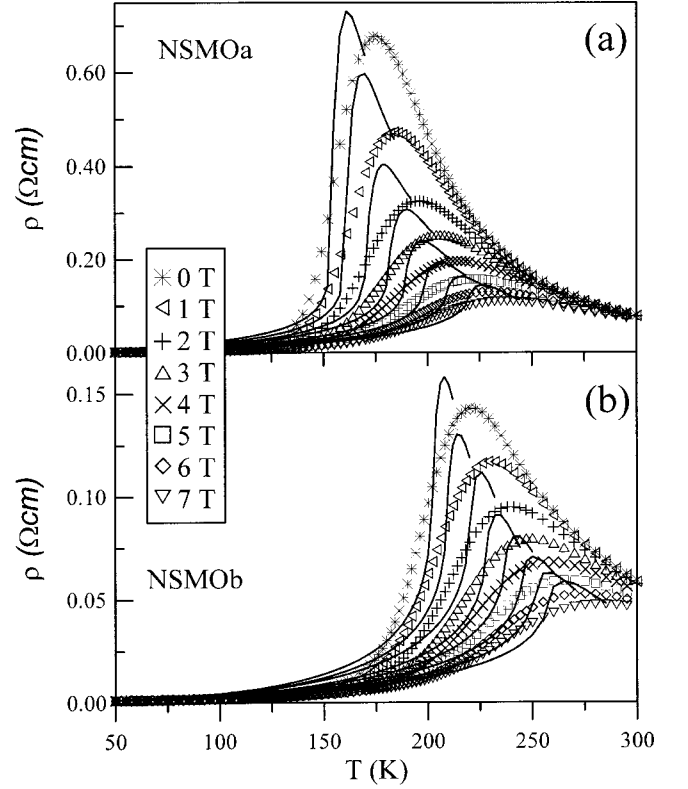


FIG. 3. Temperature dependence of resistivities for (a) NSMOa and (b) NSMOb in various magnetic fields. Solid lines are the fitted curves by Eq. (6).

zation. Because  $M = \chi(T)H$  for  $T > T_c$ , a dominant  $H^2$  contribution in MR is also generally observed.<sup>1,26</sup> Examining this behavior, one can see in Eq. (4) that the field dependence of MR is due only to the field-dependence of carrier density, as described by Eq. (3). In the PM state, the normalized magnetization  $\sigma$  is very small and, therefore, is comparable with  $h$  (i.e.,  $h$  is not negligible). Furthermore, one can easily find that  $e^{-2\delta/t} \cosh^2[(\sigma+h)/t] \ll 2x < 1$  in Eq. (3) as the temperature is raised to be larger than  $T_c$ . Thus, the term in the braces of Eq. (3) will be approximately reduced to be a constant and the field dependence of carrier density is proportional to  $\cosh[(\sigma+h)/t]$ .

Taking into account that  $(\sigma+h)/t = (J_{pd}S\chi H/M_{\max} + 2\mu_B H)/2k_B T \ll 1$ , and  $\rho \propto n^{-1}$ , we obtain  $\rho(H) \approx \rho(0) \cosh^{-1}[(J_{pd}S\chi/M_{\max} + 2\mu_B)/2k_B T H]$ . Typically we have  $\chi H/M_{\max} \leq 10^{-3}$  for  $T \gg T_c$ , and  $J_{pd}S \approx \lambda_2(7 T) \approx 1400-2100$  K. Hence, one can make an approximation and obtain

TABLE I. Fitting parameters for resistivity as described in the text.

Sample	$\rho_0$ $10^{-3} \Omega \text{ cm}$	$\lambda_1$ K	$\lambda_2$ (0 T) K	$\lambda_2$ (7 T) K	$\lambda_3$ (0 T) K	$\lambda_3$ (7 T) K	$\lambda_4$ K	$C$ $10^{-6} \Omega \text{ cm K}^{-1}$	$E_\rho$ K
NSMOa	1.45	1280	1154	1410	153	220	85	3.72	1291
NSMOb	0.98	1254	1606	1672	202	257	95	5.09	1102
LCMO	0.12	1236	2100	2120	232	275	90	0.59	1262
LSMO	0.39	1068	1756	1860	334	366	35		

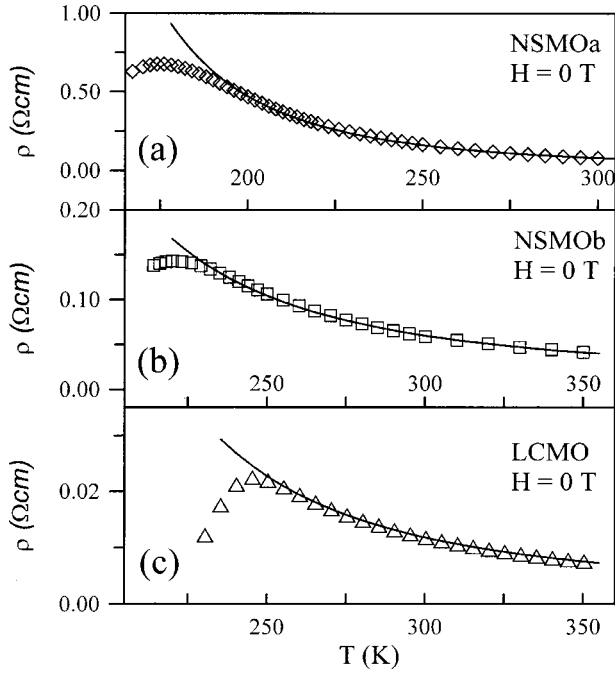


FIG. 4. The zero-field resistivities of (a) NSMOa, (b) NSMOb, and (c) LCMO films. Solid lines are the fitted curves by Eq. (5).

$$\rho(H) \approx \rho(0) \left[ 1 - \frac{1}{8} \left( \frac{J_{pd} S \chi / M_{\max} + 2\mu_B}{k_B T} \right)^2 H^2 \right], \quad (7)$$

for  $T$  at high temperatures according to  $\cosh^{-1} X \approx (1 + X^2/2)^{-1} \approx 1 - X^2/2$ , if  $X \ll 1$ .

As a consequence, the negative MR,

$$[\rho(0) - \rho(H)]/\rho(0) \approx \frac{1}{8} \left( \frac{J_{pd} S \chi / M_{\max} + 2\mu_B}{k_B T} \right)^2 H^2,$$

is obtained. In Fig. 5, we show  $[\rho(0) - \rho(H)]/\rho(0)$  vs  $H^2$  for the NSMOb sample in the PM regime. The straight lines correspond to a linear fit:  $[\rho(0) - \rho(H)]/\rho(0) = \beta H^2$ , where  $\beta$  is the slope, which is temperature dependent. Clearly, a strong  $H^2$  dependence of  $[\rho(0) - \rho(H)]/\rho(0)$  is observed for NSMOb at temperatures above 300 K. For temperatures below 290 K, however, the  $H^2$  dependence of  $[\rho(0) - \rho(H)]/\rho(0)$  holds only in the low-field region. This deviation from the linear behavior for  $[\rho(0) - \rho(H)]/\rho(0)$  in high fields is attributable to the nonlinear field dependence of  $M$  in high fields when temperature is near  $T_c$ .<sup>28</sup> To investigate the temperature dependence of  $\beta$ , we plot  $\beta$  vs  $T$  as shown in the inset of Fig. 5. According to Eq. (7) and taking into account  $\chi \propto 1/(T - T_c)$ , we predict that the term  $\beta^{0.5} \times T$  will be in proportion to  $1/(T - T_c)$ . Also shown in the inset of Fig. 5 is the  $\beta^{0.5} \times T$  vs  $1/(T - T_c)$  plot. It can be seen that a straight line well fits the data, which is in accord with our deduction. Moreover, if the applied field is not large or the magnetization is not small at temperatures not far from  $T_c$ , the term of  $\mu_B H$  is negligible and the negative MR,

$$[\rho(0) - \rho(H)]/\rho(0) \approx \frac{1}{8} \left( \frac{J_{pd} S / M_{\max}}{k_B T} \right)^2 (\chi H)^2 \propto M^2,$$

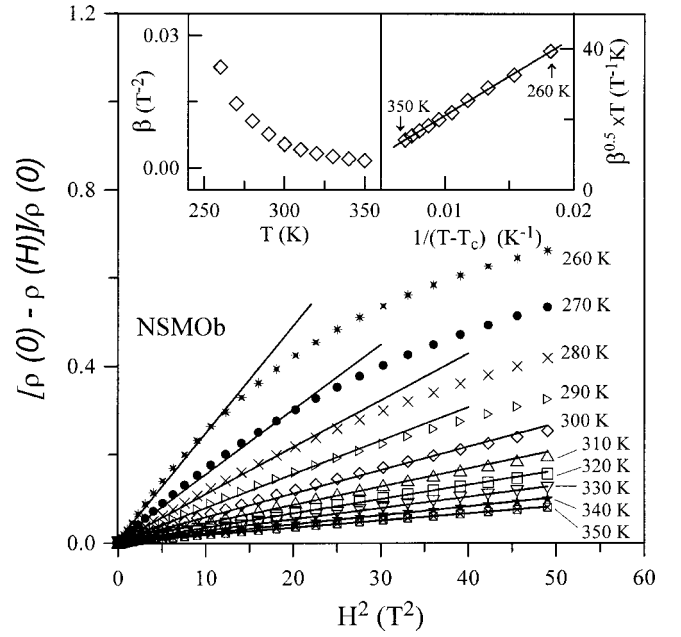


FIG. 5. Negative MR as a function of  $H^2$  for the NSMOb films. The straight lines correspond to a linear fit:  $[\rho(0) - \rho(H)]/\rho(0) = \beta H^2$ . The insets show the temperature dependence of  $\beta$  and the  $\beta^{0.5} \times T$  vs  $1/(T - T_c)$  plot.

will be expected. As previously stated, it has been reported that the electrical resistivity and the magnetization can be approximately described by the relationship  $[\rho(0) - \rho(H)]/\rho(0) = B[M(H)/M_{\max}]^2$  for the doped manganites in the low- $M$  region. Several theoretical models<sup>29,30</sup> have been proposed to investigate the nature of the  $\rho$ - $M$  correlation and show that the coefficient  $B$  is related to the coupling between moving carriers and the localized spins. The calculated value of  $B$  is about 4–5 in the case of the strong coupling, but becomes  $B \approx 1$  in the weak coupling limit.<sup>29</sup> Several experimental investigations have reported that  $B = 0.66$ –1.7 for  $\text{La}_{0.7-x}\text{Y}_x\text{Ca}_{0.3}\text{MnO}_3$ ,<sup>26</sup> and  $B = 1$ –4 for  $\text{La}_{1-x}\text{Ca}_x\text{MnO}_3$ .<sup>1</sup> It is also interesting that the parameter  $B$  seems to be independent of temperature for  $\text{La}_{0.7-x}\text{Y}_x\text{Ca}_{0.3}\text{MnO}_3$  while a weak temperature dependence of  $B$  can be observed in  $\text{La}_{1-x}\text{Ca}_x\text{MnO}_3$  samples. According to our deduction from Eq. (7), the parameter  $B$  is approximately estimated by  $B = (J_{pd} S / k_B T)^2 / 8$ . Taking  $J_{pd} S = 1672$  K for the NSMOb sample and  $T = 350(300)$  K, we obtain  $B \approx 2.9(3.9)$ , which is comparable to that reported by others. We can also draw an inference that the parameter  $B$  should be weakly dependent of  $T$  in the high-temperature region for the manganites with a low  $J_{pd} S$  value. The temperature dependence of  $B$  remains to be clarified.

#### IV. CONCLUSION

In conclusion, we have derived an expression of resistive behavior for the CMR manganites based on the CCDC theory. Our low-temperature resistivity data on high-quality epitaxial thin films of doped Mn oxides can be well fitted by the derived  $\rho(T)$  equation. For  $T$  above  $T_c$ , the zero-field resistivity data can be also well explained by the CCDC

model. Furthermore, the dominant  $T^2$  contribution in low-temperature resistivity, and the strong  $H^2$  dependence of magnetoresistance at temperatures above  $T_c$  are successfully interpreted in accordance with our deduction. We have provided strong evidence to suggest that current-carrier-density collapse is the origin of CMR.

### ACKNOWLEDGMENT

The authors thank the National Science Council of the Republic of China for financial support under Grants Nos. NSC 89-2112-M-212-002 and NSC 89-2112-M-002-072.

- 
- <sup>1</sup>A. Urushibara, Y. Moritomo, T. Arima, A. Asamitsu, G. Kido, and Y. Tokura, *Phys. Rev. B* **51**, 14 103 (1995).
- <sup>2</sup>G. J. Snyder, R. Hiskes, S. DiCarolis, M. R. Beasley, and T. H. Ge, *Phys. Rev. B* **53**, 14 434 (1996).
- <sup>3</sup>M. Jaime, P. Lin, M. B. Salamon, and P. D. Han, *Phys. Rev. B* **58**, 5901 (1998).
- <sup>4</sup>T. Akimoto, Y. Moritomo, and A. Nakamura, *Phys. Rev. Lett.* **85**, 3914 (2000).
- <sup>5</sup>R. M. Kusters, J. Singleton, and D. A. Keen, *Physica B* **155**, 361 (1989).
- <sup>6</sup>G. Jakob, W. Westerburg, F. Martin, and H. Adrian, *Phys. Rev. B* **58**, 14 966 (1998).
- <sup>7</sup>M. Viret, L. Ranno, and J. M. D. Coey, *Phys. Rev. B* **55**, 8067 (1997).
- <sup>8</sup>L. Sheng, D. Y. Xing, D. N. Sheng, and C. S. Ting, *Phys. Rev. Lett.* **79**, 1710 (1997).
- <sup>9</sup>M. Kataoka, *Phys. Rev. B* **63**, 134435 (2001).
- <sup>10</sup>A. S. and A. M. Bratkovsky, *Phys. Rev. Lett.* **82**, 141 (1999).
- <sup>11</sup>Guo-meng Zhao, Y. S. Wang, D. J. Kang, W. Prellier, M. Rajeswari, H. Keller, T. Venkatesan, C. W. Chu, and R. L. Greene, *Phys. Rev. B* **62**, 11 949 (2000); Zhao, Guo-meng, *ibid.* **62**, 11 639 (2000).
- <sup>12</sup>Guo-meng Zhao, D. J. Kang, W. Prellier, M. Rajeswari, H. Keller, T. Venkatesan, and R. L. Greene, *Phys. Rev. B* **63**, 060402 (2001).
- <sup>13</sup>J. R. Simpson, H. D. Drew, V. N. Smolyaninova, Greene, R. L., Robson, M. C., Biswas, A., and Rajeswari, M., *Phys. Rev. B* **60**, 16 263 (1999).
- <sup>14</sup>Guo-meng Zhao, V. Smolyaninova, W. Prellier, and H. Keller, *Phys. Rev. Lett.* **84**, 6086 (2000).
- <sup>15</sup>A. S. Alexandrov and A. M. Bratkovsky, *J. Appl. Phys.* **85**, 4349 (1999).
- <sup>16</sup>X. Liu, X. Xu, and Y. Zhang, *Phys. Rev. B* **62**, 15 112 (2000).
- <sup>17</sup>S. L. , W. Y. Zhao, G. Q. Zhang, F. Tu, G. Peng, J. Liu, Y. P. Yang, G. Li, Y. Jiang, X. Y. Zeng, C. Q. Tang, and S. Z. Jin, *Appl. Phys. Lett.* **77**, 4398 (2000).
- <sup>18</sup>D. Emin and T. Holstein, *Ann. Phys. (N.Y.)* **53**, 439 (1969).
- <sup>19</sup>M. Ziese and C. Srinithiwarawong, *Phys. Rev. B* **58**, 11 519 (1998).
- <sup>20</sup>L. M. Wang, H. H. Sung, B. T. Su, H. C. Yang, and H. E. Horng, *J. Appl. Phys.* **88**, 4236 (2000).
- <sup>21</sup>H. J. Lee, J. H. Jung, Y. S. Lee, J. S. Ahn, T. W. Noh, K. H. Kim, and S-W. Cheong, *Phys. Rev. B* **60**, 5251 (1999).
- <sup>22</sup>T. Okuda, Y. Tomioka, A. Asamitsu, and Y. Tokuru, *Phys. Rev. B* **61**, 8009 (2000).
- <sup>23</sup>K. H. Kim, J. H. Jung, and T. W. Noh, *Phys. Rev. Lett.* **81**, 1517 (1998).
- <sup>24</sup>R. H. Heffner, L. P. Le, M. F. Hundley, J. J. Neumeier, G. M. Luke, K. Kojima, B. Nachumi, Y. J. Uemura, D. E. MacLaughlin, and S-W. Cheong, *Phys. Rev. Lett.* **77**, 1869 (1996).
- <sup>25</sup>A. S. Alexandrov and A. M. Bratkovsky, *J. Phys.: Condens. Matter* **11**, 1989 (1999).
- <sup>26</sup>J. Fontcuberta, B. Martínez, A. Seffar, S. Piñol, J. L. García-Muñoz, and X. Obradors, *Phys. Rev. Lett.* **76**, 1122 (1996).
- <sup>27</sup>J. O'Donnell, M. Onellion, M. S. Rzchowski, J. N. Eckstein, and I. Bozovic, *Phys. Rev. B* **54**, 6841 (1996).
- <sup>28</sup>P. Matl, N. P. Ong, Y. F. Yan, Y. Q. Li, D. Studebaker, T. Baum, and G. Doubinina, *Phys. Rev. B* **57**, 10 248 (1998).
- <sup>29</sup>N. Furukawa, *J. Phys. Soc. Jpn.* **63**, 3214 (1994).
- <sup>30</sup>J. Inoue and S. Maekawa, *Phys. Rev. Lett.* **74**, 3407 (1995).